Available online at www.sciencedirect.com
ScienceDirect
Journal of the European Ceramic Society 29 (2009) 1463–1468
www.elsevier.com/locate/jeurceramsoc

Thermal expansion behaviour of Sr- and Mg-doped $LaGaO_3$ solid electrolyte

Pradyot Datta [a,c,*], Peter Majewski [b], Fritz Aldinger [c]

[a] Technische Universität Clausthal, Institut für Metallurgie, 42 Robert-Koch Strasse, 38678 Clausthal-Zellerfeld, Germany
[b] University of South Australia, School of Advanced Manufacturing and Mechanical Engineering, Mawson Lakes, South Australia 5095, Australia
[c] Max-Planck-Institut für Metallforschung, Pulvermetallurgisches Laboratorium, Heisenbergstrasse 3, Stuttgart 70569, Germany

Received 6 February 2008; received in revised form 18 August 2008; accepted 28 August 2008
Available online 11 November 2008

Abstract

Thermal expansion coefficients (TECs) of Sr- and Mg-doped $LaGaO_3$ were measured continuously from room temperature up to 1000 °C. It was observed that TECs increased with the increase in dopant concentration. In the continuous TEC curve depression due to a structural change from orthorhombic to rhombohedral of the material was also observed. It was found that at a given Sr content varying the amount of Mg content led to an increase in the phase transformation temperature whereas the reverse was found to be true with the increase in Sr content. The thermal expansion was found to increase with increasing oxygen vacancies irrespectively of the type of the dopant responsible for causing the vacancy. This increase was attributed to the weakening of the binding energy as a result of the creation of additional oxygen vacancies.

Keywords: Powders-solid state reaction; Thermal expansion; Perovskites; Fuel cells; $LaGaO_3$

1. Introduction

Strontium and/or magnesium doped lanthanum gallate ($LaGaO_3$) ceramics are promising electrolyte materials for solid oxide fuel cells because of their superior oxygen ion conducting properties over a wide range of oxygen partial pressure. While the cell performance of $La_{1-x}Sr_xGa_{1-y}Mg_yO_{3-\delta}$ (LSGM, where $\delta = (x+y)/2$) and conductivity data and other properties of this group of materials are reported,[1–5] the thermal expansion coefficient (TEC) data are surprisingly not well documented.

Given the fact that a solid oxide fuel cell is composed of different materials functioning as a cathode, anode, solid electrolyte and interconnect, respectively, it can be considered as a classical example of composite material. Since such composites are used at high temperatures, it is necessary that all their components have matching TECs in the temperature range of interest. Otherwise, there is a risk of fracturing the composite. Thus, TECs of the materials are important for the practical design of their use at high temperatures. As the thermal expansion of inorganic materials is often expressed with a polynomial series of temperature having no physical meaning, it is not proper to extrapolate the expansion value beyond the measured range.

The knowledge of actual TEC data is important because $LaGaO_3$ is polymorphic having orthorhombic structure at room temperature and it transforms to a rhombohedral symmetry at around 148 °C.[6–8] The average TEC of Sr- and Mg-doped $LaGaO_3$ has been investigated by various researchers.[9–11] Ishihara et al.[12] measured the TEC of $La_{0.9}Sr_{0.1}Ga_{0.8}Mg_{0.2}O_{2.85}$ between room temperature and 1000 °C and found that it is similar to that of yttria stabilized zirconia. However, they could not find any phase transition in doped $LaGaO_3$ in this temperature range. Recently Hayashi et al.[13] reported about the TEC behaviour of doped $LaGaO_3$ as a function of temperature, but they have not taken the crystal structures of the different compositions into account. However, Datta et al.[14] have shown orthorhombic, orthorhombic + rhombohedral and cubic crystal structures of doped $LaGaO_3$ depending on the amount of dopant concentration.

It is noted that the symmetry of ABO_3 type perovskite materials is very much dependent upon the extent of edge sharing

* Corresponding author at: Technische Universität Clausthal, Institut für Metallurgie, 42 Robert-Koch Strasse, 38678 Clausthal-Zellerfeld, Germany. Tel.: +49 5323 723688; fax: +49 5323 723184.
E-mail address: pdatta@rediffmail.com (P. Datta).

0955-2219/$ – see front matter © 2008 Elsevier Ltd. All rights reserved.
doi:10.1016/j.jeurceramsoc.2008.08.029

oxygen octahedra. In the ideal structure, where the atoms are touching one another, the B–O distance is equal to $a/2$ (a is the cubic atomic cell parameter) while the A–O distance is $a/\sqrt{2}$ and the relationship between the ionic radii holds: $r_A + r_O = \sqrt{2}(r_B + r_O)$. The cubic structure is normally retained even if there is a slight deviation from this relation. As a measure of the deviation from the ideal situation, Goldschmidt[15] introduced a tolerance factor (t) defined by:

$$t = \frac{r_A + r_B}{\sqrt{2}(r_B + r_O)}$$

which is applicable at room temperature to the empirical ionic radii of the constituents. Although for an ideal structure t is unity, this structure is also found for lower t values ($0.75 < t < 1.0$). Deviations from the ideal structure with orthorhombic, rhombohedral, tetragonal, monoclinic and triclinic symmetry are known, although the latter three are scarce and poorly characterized. The distorted structure may exist at room temperature, but it transforms to the cubic structure at high temperatures. This transition may occur in several steps through intermediate distorted phases. These deviations from the cubic perovskite structure may proceed from a simple distortion of the cubic unit cell or an enlargement of the unit cell or a combination of the both. This distortion and tilt is also dependent on the size of A and B site cations. Thus, it is necessary to consider the phase transition of LSGM, which belongs to perovskite group, while measuring the TEC.

In the present study, the TEC of Sr- and Mg-doped $LaGO_3$ with systematically changed dopant contents are measured and the doping effect is discussed in terms of the oxygen vacancy, taking into account the individual crystal structures.

2. Experimental procedure

The samples were prepared by solid state synthesis starting from powders of La_2O_3 (99.99%, Sigma–Aldrich, Steinheim, Germany), $SrCO_3$ (98%+, Sigma–Aldrich, Steinheim, Germany), Ga_2O_3 (99.99%, Sigma–Aldrich, Steinheim, Germany) and MgO (98%+, Merck, Darmstadt, Germany). The powders were first dried at 130 °C for 3 h in air then weighed and mixed in appropriate amounts to get the individual overall nominal compositions. The powder mixtures were thoroughly mixed by milling in a zirconia ball mill for half an hour and then calcined at 1200 °C for 24 h in air, subsequently milled for half an hour and then finally calcined at 1400 °C for 24 h in air. The calcined powder was then milled for 2 h to obtain a homogeneous powder with a particle size of few microns. The powder mixtures were then isostatically cold pressed at 625 MPa for 60 s into rectangular compacts with the dimension of 15 mm × 5 mm × 5 mm. The pressed samples were then sintered at 1500 °C for 12 h at a static air atmosphere. Heating rate for all cases were 5 °C/min and all samples were furnace cooled to room temperature. In this text the following nomenclature will be followed, for example, $La_{1-x}Sr_xGa_{1-y}Mg_yO_{3-\delta}$ will be referred as LSGM xy for the sake of convenience.

2.1. Sample characterization

The TEC measurement was carried out in air using a push rod type differential dilatometer (Model 802, Bähr-Thermoanalyse GmbH, Hüllhorst, Germany) in the temperature range from room temperature to 1000 °C. A bar of sapphire of the dimension of 10 mm × 4 mm × 4 mm was used as the reference sample. Measurements were performed at a heating and cooling rate of 3 °C/min. TEC (α) is generally expressed by:

$$\alpha = \frac{dL/dT}{L}$$

Since data of length and temperature are both functions of time, the above expression can be written as

$$\alpha = \frac{(dL/dt)/(dT/dt)}{L}$$

where L is the length of a sample at room temperature and dt is the time interval of the sampling. Data of differential length and temperature was acquired every second and differential thermal expansion (dL/dt) was calculated after smoothening the data.

Differential scanning calorimetry (DSC) (Model STA 449C, NETZSCH-Gerätebau GmbH, Selb, Germany) of some selective samples were carried out using around 50 mg of powder. Samples were heated in an alumina crucible up to 900 °C with a heating rate of 3 °C/min. Chosen atmosphere was a mixture of argon with 20% O_2.

3. Results

Fig. 1 shows the thermal expansion of $LaGaO_3$ (LG), $La_{0.9}Sr_{0.1}GaO_{3-\delta}$ (LSG 10), $LaGa_{0.9}Mg_{0.1}O_{3-\delta}$ (LGM 10) and $LaGa_{0.8}Mg_{0.2}O_{3-\delta}$ (LGM 20). Abnormalities of the thermal expansion for LG and LSG10 can be seen at around 148 °C. It is also observed that the thermal expansion is higher when Mg substitutes Ga. In Figs. 2–4, the TEC curves of LG with varying amounts of Mg and a fixed Sr content are shown. It is observed in the above figures that TEC increases gradually

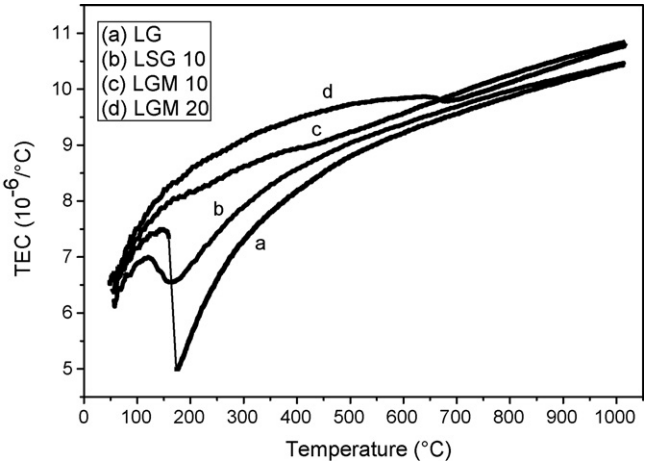

Fig. 1. TEC of $LaGaO_3$ with either A or B site dopants as a function of temperature. (a) $LaGaO_3$, (b) $La_{0.9}Sr_{0.1}GaO_{3-\delta}$, (c) $LaGa_{0.9}Mg_{0.1}O_{3-\delta}$, and (d) $LaGa_{0.8}Mg_{0.2}O_{3-\delta}$.

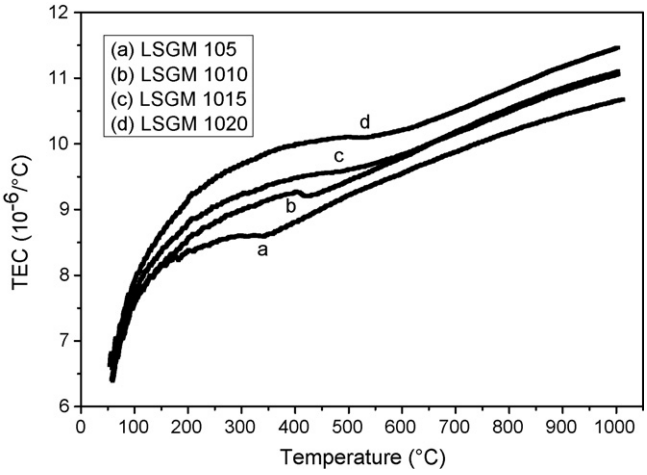

Fig. 2. Variation of TEC of $La_{0.9}Sr_{0.1}Ga_{1-y}Mg_yO_{3-\delta}$ with temperature. (a) $y = 0.05$, (b) $y = 0.10$, (c) $y = 0.15$, and (d) $y = 0.20$.

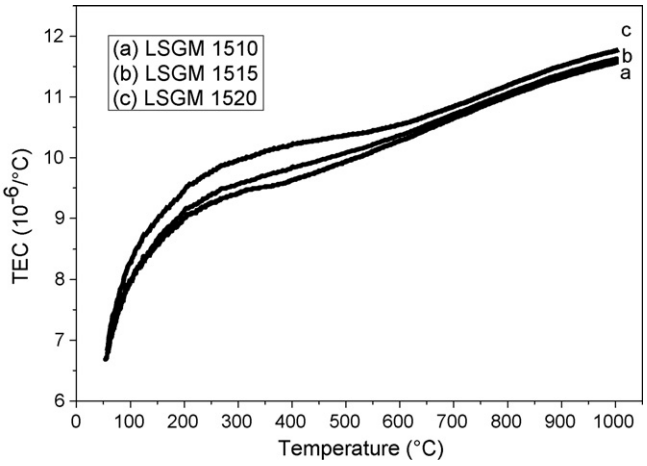

Fig. 3. Variation of TEC of $La_{0.85}Sr_{0.15}Ga_{1-y}Mg_yO_{3-\delta}$ with temperature. (a) $y = 0.10$, (b) $y = 0.15$, and (c) $y = 0.20$.

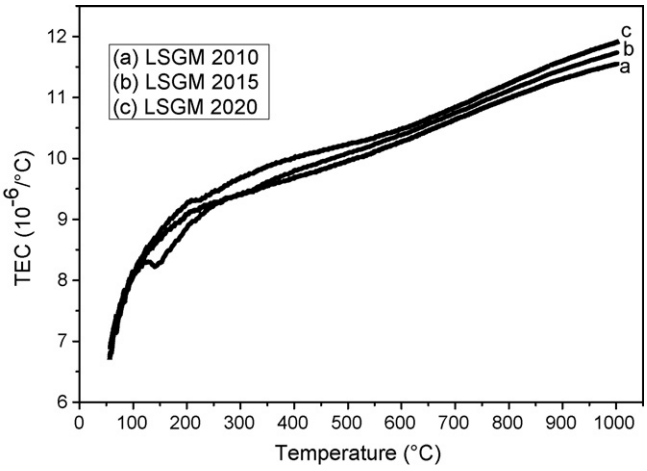

Fig. 4. Variation of TEC of $La_{0.80}Sr_{0.20}Ga_{1-y}Mg_yO_{3-\delta}$ with temperature. (a) $y = 0.10$, (b) $y = 0.15$, and (c) $y = 0.20$.

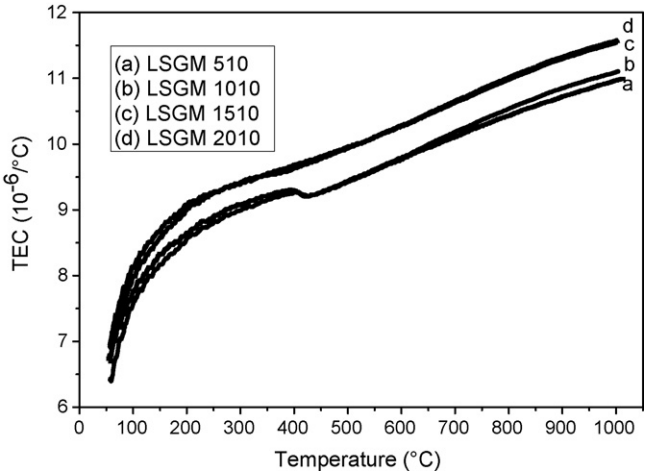

Fig. 5. Variation of TEC of $La_{1-x}Sr_xGa_{0.9}Mg_{0.1}O_{3-\delta}$ with temperature. (a) $x = 0.05$, (b) $x = 0.10$, (c) $x = 0.15$, and (d) $x = 0.20$.

with increasing amount of Mg dopant. A significant point to be noted here is the fact that an increase of the Mg content causes the abnormalities in the TEC to shrink and to become broader. Also, it is observed that the transition temperature of the abnormality increases with the increase of Mg content. However, when the results of Figs. 2 and 3 are compared it is readily visible that the transition temperature has become even broader. However, when the Sr content is increased further (Fig. 4) it is noticed that the abnormality in the TEC curve reappears (Fig. 4, line a) when the Mg content is low. Only when the Mg content is increased simultaneously, the transition point again moves to the higher temperature and becomes broader. In Fig. 5, the effect of Sr doping on the TEC curve of LSGM at a fixed Mg content is depicted. It is found that TEC increases with increasing amount of Sr content. It is also noticed that there is little or no difference in TEC when the increment of dopant is small. In Figs. 6 and 7, the Sr content has been varied again, keeping the Mg content at 15 and 20 at.%, respectively. In this case the trend is similar, i.e. TEC increases with the increase of dopant content. Although it is difficult to pin point the exact

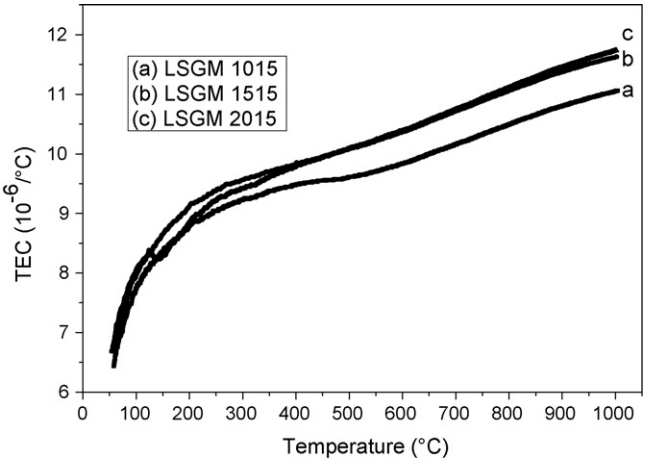

Fig. 6. Variation of TEC of $La_{1-x}Sr_xGa_{0.85}Mg_{0.15}O_{3-\delta}$ with temperature. (a) $x = 0.10$, (b) $x = 0.15$, and (c) $x = 0.20$.

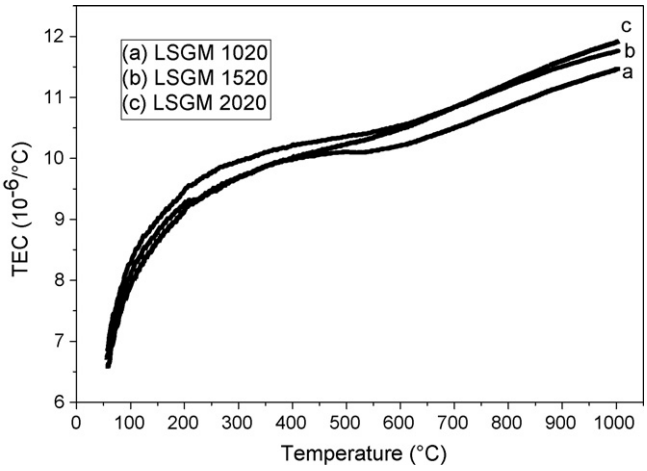

Fig. 7. Variation of TEC of $La_{1-x}Sr_xGa_{0.80}Mg_{0.20}O_{3-\delta}$ with temperature. (a) $x = 0.10$, (b) $x = 0.15$, and (c) $x = 0.20$.

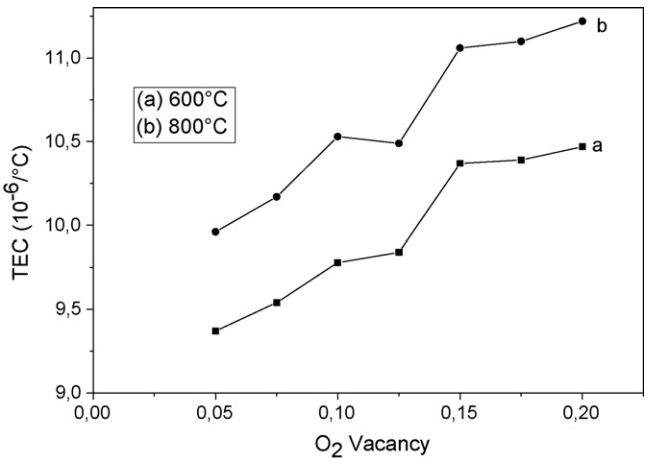

Fig. 8. Variation of TEC as a function of O_2 non-stoichiometry (δ).

transition temperature from the TEC curves other than that of LG, the lowest data point has been taken as the transition temperature and is given in Table 1. It is noted here that earlier findings[14] indicate some compositions like LSGM 1020, LSGM 1515 and LSGM 2010 to possess a mixed orthorhombic and rhombohedral structure. Thus, the given transition point should be taken as transformation from the pseudo-orthorhombic to the rhombohedral structure for the above mentioned compositions. It is noticed from Table 1 that the transformation temperature increases with Mg doping but decreases with Sr doping. It is interesting to note that LSGM 2015, LSGM 1520 and LSGM 2020 [Figs. 6 and 7, Fig. 6, line c and Fig. 7, lines b and c] samples do not show any transition point in their TEC curves.

As the intended operation temperature of SOFC is between 600 and 800 °C, the absolute value of TEC between 600 and 800 °C is shown in Fig. 8 as a function of the oxygen vacancy δ which arises irrespective of A or B site doping by Sr and Mg, respectively. Factor δ was calculated using electro-neutrality condition. It is observed from Fig. 8 that the TEC linearly increases with the increase of the oxygen vacancy. Also, as expected, at higher temperatures TEC has higher values than at lower temperatures. The DSC curves of some selected samples clearly indicate that LG exhibits a pronounced endothermic peak at about 150 °C, whereas, LSGM 2020 does not (Fig. 9).

Table 1
Orthorhombic to rhombohedral phase transformation temperature (T_C) of different $La_{1-x}Sr_xGa_{1-y}Mg_yO_{3-\delta}$ compositions.

Sample	T_C (°C)
LG	148
LSG 10	134
LGM 10	359
LGM 20	655
LSGM 510	403
LSGM 1010	402
LSGM 1510	316
LSGM 2010	239
LSGM 105	333
LSGM 1015	407
LSGM 1020	420
LSGM 1515	356

4. Discussion

The samples were sintered at 1500 °C because of the assumption that at this temperature the diffusivity of the constituents was high enough so as to form the equilibrium phases. It is also assumed that furnace cooling was fast enough to avoid reaction by long distance diffusion and only polymorphic transformations were expected to occur during cooling. Strictly speaking all investigated samples were metastable by nature. Rozumek et al.[16] found that at around 1100 °C, the solubility of Sr and Mg was close to zero. This thermodynamic limitation forces to prepare samples at high temperatures and to cool sufficiently fast in order to retain the phases which formed at high temperature after cooling.

Electrostatic attraction and repulsion forces within the lattice of a material namely lattice energy, determine the thermal expansion of the material. These forces are the function of the

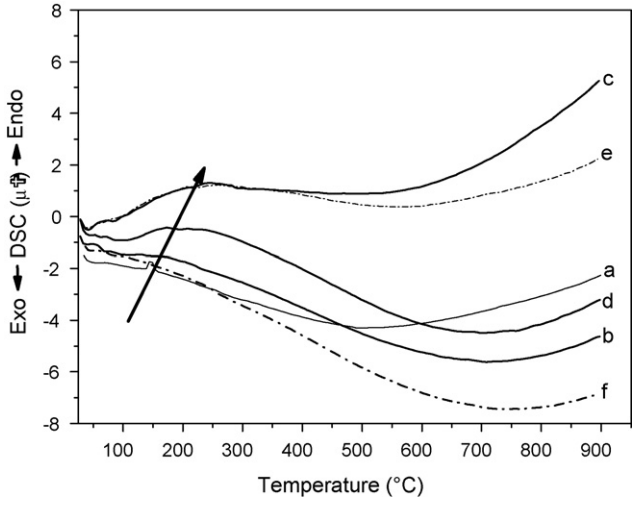

Fig. 9. DSC curves of (a) LG, (b) LSG 10, (c) LGM 10, (d) LSGM 1010, (e) LSGM 1515, and (f) LSGM 2020.

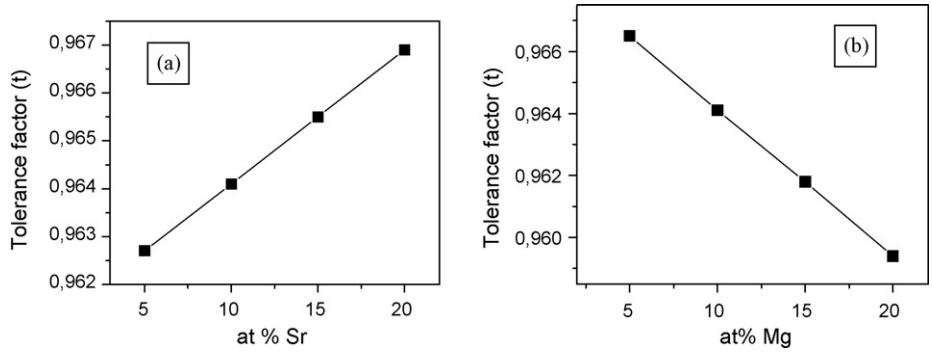

Fig. 10. Variation of the calculated Goldschmidt's tolerance factor (t) with (a) increasing Sr content in $LaGa_{0.9}Mg_{0.1}O_{3-\delta}$ and (b) with increasing Mg content in $La_{0.9}Sr_{0.1}GaO_{3-\delta}$.

positive and negative charges and their locations in the lattice. The thermal expansion increases if the attraction forces decrease. For a definite crystal structure and at a fixed oxygen/metal stoichiometric composition, the TEC is characterized only by the lattice vibrations.[17] However, if there is loss of oxygen due to an increase in temperature or due to a reducing atmosphere then thermal expansion will be increased. Doping of Sr and Mg incorporates oxygen vacancies in the parent lattice of $LaGaO_3$. So, an increase in TEC is expected. Further, the substitution of the larger Mg cation for the smaller Ga cation increases the weighted average radius of B site cation, which in turn decreases the Goldschmidt's factor t, as can be seen from the Fig. 10(b). The atomic radii of the elements, which are taken from literature[18] are given in Table 2. The substitution of Ga by Mg enlarges the BO_6 octahedra locally and the tilting of BO_6 octahedra in the doped $LaGaO_3$ becomes larger than that of GaO_6 octahedra. The larger tilting of the BO_6 octahedra may restrict the rearrangement of the octahedra during the phase transition. This is the reason why Mg doping increases the transition temperature. In contrast with Mg doping, Sr doping for the La site, decreases the transition temperature. Fig. 10(a) shows calculated t values with the variation of the Sr content. It implies that increasing t decreases the tilting of the BO_6 octahedra by doping. This may be the reason for the decrease of transformation temperature with increasing Sr doping.

There is a definite change in the distortion of the perovskite with Sr and Mg doping as their atomic radii are different from that of La and Ga, respectively. Consequently, in case of $LaGaO_3$, the angle between Ga–O–Ga, which is the measure of angles between the neighbouring oxygen octahedra, has to change with increasing Sr and Mg dopant contents. Different phase modification of $LaGaO_3$ with the increase in Sr and Mg dopant is a direct result of the change of the degree of tilt and distortion of the oxygen octahedra.

LSGM 1520, LSGM 2020 and LSGM 2015 do not show any transition temperature because the structures of these compositions are cubic at room temperature. This is consistent with the findings from the XRD studies.[14] However, this does not agree with Hayashi et al.[13] They found a transformation even in the above mentioned compositions too. It is rather overestimation to consider all compositions of LSGM as orthorhombic at room temperature. Other than that, the present result matches well with them. Literature reports concerned with the TEC of Sr- and Mg-doped $LaGaO_3$ oxides, as the temperature derivative of thermal expansion, are limited to that of Hayashi et al.[13] though there are some reports on the average TEC values as mentioned before. Therefore, there are not enough reference data to be compared with our results. TEC of LSGM 2020 at 600 °C is reported to be $11.57 \times 10^{-6}\,°C^{-1}$,[13] whereas, the value obtained by the present study is $10.47 \times 10^{-6}\,°C^{-1}$. This difference is attributed to the presence of appreciable amount of the secondary phase $LaSrGa_3O_7$[19] which has lower TEC value than that of LSGM.[20] As a consequence, in the present study, the average TEC value of LSGM 2020 is found to be lower than that reported in the literature. However, the transformation temperature obtained from the TEC curves and that of DSC is in good agreement and fall within ±10 °C. As the DSC curves also do not show any sharp transition point, rather a gradual transition (Fig. 10), a comparison is done by a manual examination of the peaks. Some authors[21,22] reported the enthalpy of formation for doped $LaGaO_3$. They found it to decrease with the content of oxygen vacancy. This means that the binding energy of doped $LaGaO_3$ becomes smaller and therefore the thermal expansion coefficient becomes larger with the increase of oxygen vacancies (Fig. 8).

Table 2
Ionic radius of the elements[18].

Element	Radius (Å)
La^{3+}(XII)[a]	1.36
Sr^{2+}(XII)	1.44
O^{2-} (VI)	1.40
Ga^{3+} (VI)	0.62
Mg^{2+}(VI)	0.72

[a] Co-ordination number.

5. Conclusion

The TEC of Sr- and Mg-doped $LaGaO_3$ was measured continuously from room temperature up to 1000 °C. $LaGaO_3$ retains orthorhombic structure even after a total dopant concentration of 25 at.%.[14] As $LaGaO_3$ transforms to rhombohedral at 148 °C, in the continuous TEC curve depression due to structural change from orthorhombic to rhombohedral of the material was also observed. It was found that there is a specific pattern in the trans-

formation temperature and the type and amount of dopant. At a given Sr content, varying the amount of Mg content increased the phase transformation temperature, but the same decreased with the increase of Sr content. The effect of doping on TEC was interpreted in terms of the oxygen vacancy created by doping. It was found that TEC increases with the increase of oxygen vacancies irrespectively to the type of dopant which is responsible for the vacancy. This increase was attributed to the weakening of the binding energy as a result of creation of oxygen vacancy.

Acknowledgement

The authors gratefully acknowledge the financial support which Pradyot Datta received from Max-Planck-Society in the form of a fellowship.

References

1. Ishihara, T., Matsuda, H. and Takita, Y., Doped-$LaGaO_3$ perovskite type oxide as a new oxide ionic conductor. *J. Am. Chem. Soc.*, 1994, **116**, 3801–3803.
2. Sandstrom, R. L., Giess, E. A., Gallagher, W. J., Segmüller, A., Cooper, E. I., Chisholm, M. F., Gupta, A., Shinde, S. and Laibowitz, R. B., Lanthanum gallate substrates for epitaxial high-temperature superconducting thin films. *Appl. Phys. Lett.*, 1998, **53**, 1874–1876.
3. Huang, K., Tichy, R. S. and Goodenough, J. B., Superior perovskite oxide-ion conductor; strontium- and magnesium-doped $LaGaO_3$. I. Phase relationships and electrical properties. *J. Am. Ceram. Soc.*, 1998, **81**, 2565–2575.
4. Wolfenstine, J., Huang, P. and Petric, A., High-temperature mechanical behavior of the solid-state electrolyte: $La_{0.8}Sr_{0.2}Ga_{0.85}Mg_{0.15}O_{2.825}$. *J. Electrochem. Soc.*, 2000, **147**, 1668–1670.
5. Datta, P., Majewski, P. and Aldinger, F., X-ray photoelectron spectroscopic study of Sr and Mg doped $LaGaO_3$ solid electrolyte surface. *Mater. Res. Bull.*, 2008, **43**, 1–8.
6. Slater, P. R., Irvine, J. T. S., Ishihara, T. and Takita, Y., High temperature powder neutron diffraction study of the oxide ion conductor $La_{0.9}Sr_{0.1}Ga_{0.8}Mg_{0.2}O_{2.85}$. *J. Solid State Chem.*, 1998, **139**, 135–143.
7. Mathews, T., Manoravi, P., Antony, M. P., Sellar, J. R. and Muddle, B. C., Fabrication of $La_{1-x}Sr_xGa_{1-y}Mg_yO_{3-(x+y)/2}$ thin films by pulsed laser ablation. *Solid State Ionics*, 2000, **135**, 397–402.
8. Marti, W., Fischer, P., Altofer, F., Scheel, H. J. and Tadin, M., Crystal structures and phase transitions of orthorhombic and rhombohedral $RGaO_3$ (R = La, Pr, Nd) investigated by neutron powder diffraction. *J. Phys.: Condens. Matter*, 1994, **6**, 127–136.
9. Ishihara, T., Matsuda, H. and Takita, Y., Effects of rare earth cations doped for La site on the oxide ionic conductivity of $LaGaO_3$-based perovskite type oxide. *Solid State Ionics*, 1995, **79**, 147–151.
10. Feng, M. and Goodenough, J. B., A superior oxide ion electrolyte. *Eur. J. Solid State Inorg. Chem.*, 1994, **31**, 663–672.
11. Stevenson, J. W., Amstrong, T. R., McCready, D. E., Pederson, L. R. and Weber, W. J., Processing and electrical properties of alkaline earth-doped lanthanum gallate. *J. Electrochem. Soc.*, 1997, **144**, 3613–3620.
12. Ishihara, T., Honda, M., Shibayama, T., Minami, H., Nishiguchi, H. and Takita, Y., Intermediate temperature solid oxide fuel cells using a new $LaGaO_3$ based oxide ion conductor. *J. Electrochem. Soc.*, 1998, **145**, 3177–3183.
13. Hayashi, H., Suzuki, M. and Inaba, H., Thermal expansion of Sr- and Mg-doped $LaGaO_3$. *Solid State Ionics*, 2000, **128**, 131–139.
14. Datta, P., Majewski, P. and Aldinger, F., Structural studies of Sr- and Mg-doped $LaGaO_3$. *J. Alloy Compd.*, 2007, **438**, 232–237.
15. Goldschmidt, V. M., Die Gesetze der Krystallochemie. *Naturwissenschaften*, 1926, **14**, 477–485.
16. Rozumek, M., Majewski, P. and Aldinger, F., Metastable crystal structure of strontium- and magnesium-substituted $LaGaO_3$. *J. Am. Ceram. Soc.*, 2004, **87**, 656–661.
17. Ullmann, H., Trofimenko, N., Tietz, F., Stöver, D. and Khanlou, A. A., Correlation between thermal expansion and oxide ion transport in mixed conducting perovskite-type oxides for SOFC cathodes. *Solid State Ionics*, 2000, **138**, 79–90.
18. Shannon, R. D., Revised effective ionic radii and systematic studies of interatomic distances in halides and chalcogenides. *Acta Crystallogr. A*, 1976, **32**, 751–767.
19. Datta, P., Majewski, P. and Aldinger, F., Synthesis and microstructural characterization of Sr- and Mg-substituted $LaGaO_3$ solid electrolyte. *Mater. Chem. Phys.*, 2007, **102**, 240–244.
20. Rozumek, M., Kristallchemische Eigenschaften ausgewählter Funktionskeramiken im quasi-quaternären system Ga_2O_3–La_2O_3–MgO–SrO. *PhD Thesis*, Stuttgart University, 2003.
21. Islam, M. S. and Davies, R. A., Atomistic study of dopant site-selectivity and defect association in the lanthanum gallate perovskite. *J. Mater. Chem.*, 2004, **14**, 86–93.
22. Cheng, J. and Navrotsky, A., Energetics of magnesium, strontium, and barium doped lanthanum gallate perovskites. *J. Solid State Chem.*, 2004, **177**, 126–133.